Seasonal and interannual variability of calcite in the vicinity of the Patagonian shelf break (38°S–52°S)

Sergio R. Signorini,[1] Virginia M. T. Garcia,[2] Alberto R. Piola,[3] Carlos A. E. Garcia,[4] Mauricio M. Mata,[4] and Charles R. McClain[5]

[1] The timing and duration of coccolithophore blooms along the Patagonian shelf break, as well as insights on the mechanisms that drive and maintain these blooms, were analyzed using time series of chlorophyll chl *a*, calcite, and sea-surface temperature (SST) derived from remote sensing data (SeaWiFS and AVHRR) and historic hydrographic data. The seasonal variability and succession of phytoplankton groups respond to light intensity and nutrient supply within the mixed layer due to seasonal changes in stratification. The early spring bloom is diatom-dominated and starts in September under nutrient-rich Malvinas waters when the mixed layer begins to shallow (<80 m), and peaks around November with mixed layer depths (MLD) less than 40 m. After nutrient depletion from the spring bloom, a coccolithophore bloom begins in November when the MLD is less than 40 m, and peaks in January when the MLD reaches its minimum (18 m) and PAR reaches its maximum intensity. **Citation:** Signorini, S. R., V. M. T. Garcia, A. R. Piola, C. A. E. Garcia, M. M. Mata, and C. R. McClain (2006), Seasonal and interannual variability of calcite in the vicinity of the Patagonian shelf break (38°S–52°S), *Geophys. Res. Lett.*, *33*, L16610, doi:10.1029/2006GL026592.

1. Introduction

[2] The Patagonian shelf off Argentina shows complex dynamic processes influenced by tides, the confluence of Brazil and Malvinas (Falkland) Currents, and the transition zone between the shelf water of various origins and the Malvinas Current waters. The Patagonian Shelf tides constitute one of the strongest regimes in the world, where a significant amount of global tidal energy is dissipated by the effect of bottom friction [*Glorioso and Flather*, 1997]. Strong vertical mixing is promoted by very energetic tidal currents, which in turn create shelf fronts associated with high chlorophyll concentrations visible by ocean color satellites [*Romero et al.*, 2006; *Saraceno et al.*, 2005]. The Brazil/Malvinas Confluence (BMC) near 39°S results from the collision of the southward Brazil Current (BC) with the Malvinas Current (MC), which is a northward

branch of the Antarctic Circumpolar Current (ACC). The MC transports cold and relatively fresh sub-Antarctic waters equatorward, and the BMC generates one of the most energetic regions of the world ocean [*Piola and Matano*, 2001]. The MC is steered by the topography of the shelf break forming a distinct oceanographic front. High phytoplankton biomass associated with the shelf-break front is attributed to nutrient input by upwelling processes [*Carreto et al.*, 1995].

[3] Previous remote sensing studies associated the Patagonian shelf-break front with occurrence of coccolithophores [*Brown and Podesta*, 1997]. Early phytoplankton samplings in the area reported the presence of the species *Emiliania huxleyi* [*Hentschel*, 1932]. More recently, *Gayoso* [1995] reported relatively high concentrations of *Emiliania huxleyi* in the northern portion of the shelf, near the La Plata River mouth. The key environmental and ecological factors controlling the blooms of these organisms are particularly illumination, mixed layer depth, and photoadaptation. Blooms of *Emiliania huxleyi* have been reported from many regions around the globe [*Iglesias-Rodríguez et al.*, 2002], especially in the North Atlantic [*Balch et al.*, 1989; *Holligan et al.*, 1993a, 1993b]. A review of the literature on the occurrence of *E. huxleyi* and environmental factors [*Smyth et al.*, 2004; *Tyrrell and Merico*, 2004] reveals that they are associated with highly stratified water, with mixed layers almost always ≤30 m, indicating a high light requirement. Concerning nutrients, this species seems to tolerate and grow well under low levels of phosphate (high N:P ratios) [*Townsend et al.*, 1994; *Tyrrell and Taylor*, 1995], presumably due to their ability to use dissolved organic phosphorus. Silicate levels can also be low during *E. huxleyi* blooms, as many times they follow diatom blooms [*Heimdal et al.*, 1994; *Holligan et al.*, 1993a, 1993b]. Oceanic strains of this species have also been shown to tolerate low concentrations of iron [*Brand*, 1991].

[4] In this paper we offer an analysis of the timing and duration of coccolithophore blooms along the Patagonian shelf break, as well as insights on the mechanisms that drive and maintain these blooms. Our analysis is based on time series of chlorophyll and calcite concentrations derived from satellite ocean color data, historical hydrographic data, and other ancillary satellite data. The percent of coccolithophore bloom pixels were detected in the study region using coccolithophore spectral thresholds that provided excellent agreement with the calcite concentration variability. Therefore, we used increases in calcite concentration as a proxy for coccolithophore blooms. In November 2004 we carried out a cruise along the high chlorophyll band in the Patagonian shelf-break to determine the phytoplankton species composition, primary production rates and the main ocean-

[1]Science Applications International Corporation, Beltsville, Maryland, USA.
[2]Department of Oceanography, Federal University of Rio Grande, Rio Grande, Brazil.
[3]Servicio de Hidrografia Naval and Universidad de Buenos Aires, Buenos Aires, Argentina.
[4]Department of Physics, Federal University of Rio Grande, Rio Grande, Brazil.
[5]NASA Goddard Space Flight Center, Greenbelt, Maryland, USA.

ographic and optical features associated with the bloom in spring. A preliminary analysis of the cruise data was performed and used to provide further insights to this study.

2. Data Sources and Methodology

[5] The calcite and chlorophyll-a time series were generated separately in two processing steps using different sets of algorithms, but both using the 4-km Sea-viewing Wide Field-of-view Sensor (SeaWiFS) global area coverage (GAC) L1A data. The calcite images were derived using the two-band algorithm for suspended calcium carbonate (also known as particulate inorganic carbon (PIC)), based on normalized water-leaving radiance (nLw) at 440 and 550 nm [*Balch et al.*, 2005; *Gordon et al.*, 2001]. The Chl *a* was obtained from nLws (443, 490, 510, and 555 nm) using the OC4v4 chlorophyll algorithm [*O'Reilly et al.*, 2000] and revised thresholds for coccolithophore masking (C. Brown, personal communication, 2006), which provide more accurate detection of coccolithophore presence. Eight-day and monthly composites were made by binning the L2 SeaWiFS products. The percent of pixels detected by the coccolithophore flag were also binned and used in conjunction with the calcite concentration time series to provide independent evidence of coccolithophore presence. Because the OC4v4 algorithm will produce spurious chlorophyll values when coccolithophore shells are present, the binning of the chlorophyll product was obtained by excluding pixels for which coccolithophores were flagged. This process precludes the estimation of presumably lower levels of chlorophyll associated with the coccolithophore blooms. To our knowledge, there is no methodology available to quantify the possible bias that is introduced to the chlorophyll concentration.

[6] The SeaWiFS time series covers the period of September 1997–October 2005, while the Advanced Very High Resolution Radiometer (AVHRR) sea-surface temperature (SST) data spans from January 1997 to December 2004. Time series of photosynthetic available radiation (PAR) were obtained using the PAR SeaWiFS algorithm [*Frouin et al.*, 1989; *Patt et al.*, 2003], and SST was obtained from monthly 4-km AVHRR Pathfinder grids from the Jet Propulsion Laboratory PODAAC. Monthly climatologies of SST, sea-surface salinity (SSS), and nutrients (NO_3, PO_4, and SiO_2) were obtained from the World Ocean Atlas 2001 [*Conkright et al.*, 2002]. Monthly mixed layer depth (MLD) climatology was obtained from the Climatological Atlas of the World Ocean [*Levitus*, 1982]. Monthly climatologies of Chl *a*, PIC, PAR, and SST were made from the available satellite products.

3. Discussion and Results

[7] Figure 1 shows monthly composites of calcite and Chl *a* for November and December 2004, and January 2005. The white polygon delimits the portion of the Patagonian shelf break from which the data were extracted for analyses. As shown in Figure 1, there are phytoplankton blooms (including calcite-producing species) that occur over the shelf at depths less than 100 m but they are not as spatially coherent and appear to be of shorter duration, thus our choice of regional domain for analyses. Note that
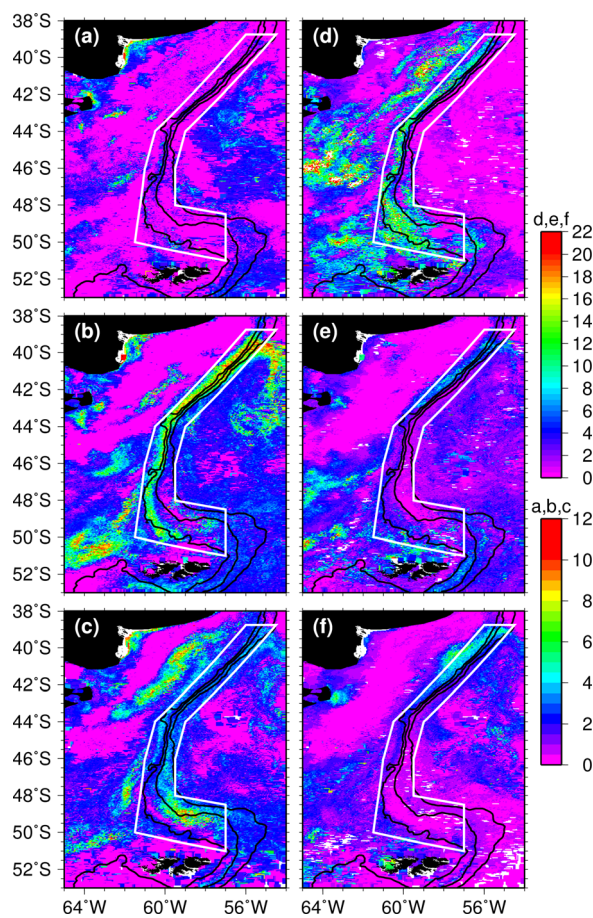
Figure 1. SeaWiFS-derived monthly composites of (a–c) calcite (in mmol C/m^3) and (d–f) chlorophyll (in mg/m^3) for November (Figures 1a and 1d), December 2004 (Figures 1b and 1e), and January 2005 (Figures 1c and 1f). The white polygon delimits the regional domain of study and the black contours correspond to the 200, 500, and 1000 m isobaths.

the Chl *a* concentrations are high (>4 mg m^{-3}) during November but are much lower (<0.5 mg m^{-3} on average) during December and January. Conversely, almost no calcite was detected within the study region in November, but significant concentrations (6 to 10 mmol C m^{-3}) were detected by the calcite algorithm during December and January. This result from ocean color data analyses was verified with the November 2004 *in situ* data. Based on preliminary analyses of these data, the distribution of phytoplankton groups across the shelf-break front showed a transition between diatom and dinoflagellate-dominated community in the front to a small size phyto-flagellate dominance east of the shelf-break front. Only a few cells of the species *Emiliania huxleyi* were detected in the shelf-break plankton samples, which likely represent the inoculum for the subsequent bloom development observed by satellite data.

[8] To demonstrate the environmental conditions conducive to phytoplankton blooms and species succession along the Patagonian shelf break, the seasonal cycle of relevant parameters is shown in Figure 2. The parameters shown in Figure 2 are monthly means of SST, SSS, MLD, NO_3, PO_4, SiO_2, Chl *a*, PIC, and PAR averaged over the regional
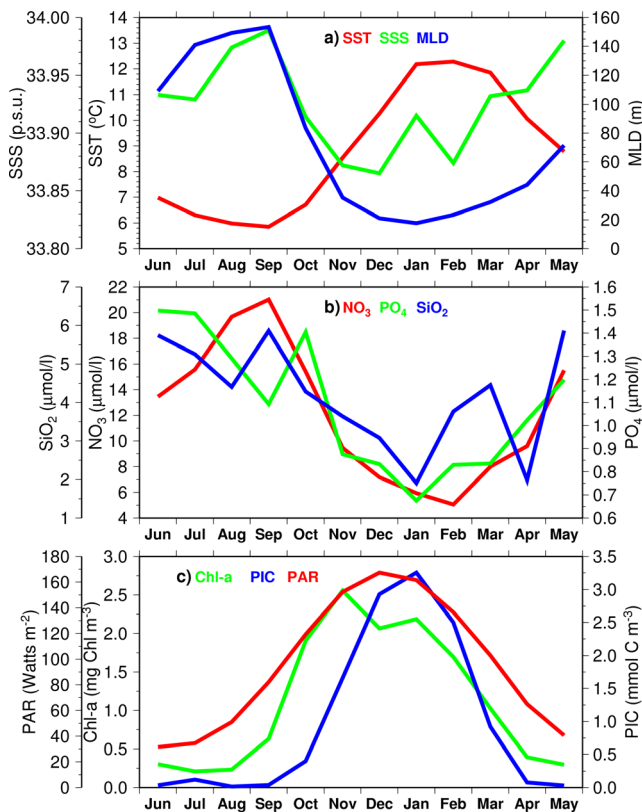
Figure 2. Seasonal cycle of mean (a) SST, SSS, MLD, (b) nutrients, (c) chlorophyll, PIC, and PAR within the regional domain defined in Figure 1.

polygon shown in Figure 1. The MLD is derived from temperature stratification alone [*Levitus*, 1982], but salinity has little effect on the calculation of the MLD as it changes very little (0.3%) throughout the year along the shelf break (Figure 2 and Table 1). The actual monthly values for each parameter are summarized in Table 1. Note that the time scale spans from June to May to place the peak PIC and Chl *a* in the center of the plot for convenience.

[9] Inspection of Figure 2 and Table 1 reveals the following seasonal progression for the physical and biogeochemical parameters. The classical spring bloom behavior starts in September when there is an increase in SST and PAR, a sharp reduction of the MLD, a subsequent reduction

in nutrient concentration due to uptake by phytoplankton during photosynthesis, and a quick rise in chlorophyll concentration. The mean Chl *a* concentration peaks in November and stays above 1.0 mg m^{-3} until March when surface PAR begins to decrease below 100 Watts/m^2 and the MLD begins to increase above 40 m. However, the calcite concentration starts to increase later in November and peaks in January when the mixed layer is shallowest (17.6 m), PAR is near a peak (161.6 Watts/m^2), and all nutrients are at their lowest concentrations and phosphate reaches its minimum value (0.68 μM). These environmental conditions, which are conducive to growth of *E. huxleyi* and are described in our analyses, closely match the conditions described in the literature (see introduction), which explains the phasing and duration of different phytoplankton blooms along the Patagonian shelf break. A community dominated by diatoms and dinoflagellates (as detected in our in situ sampling in spring) is replaced by lower biomass coccolithophores dominance as predicted in phytoplankton succession models [*Margalef*, 1978].

[10] Figure 3 shows satellite-derived time series of Chl *a*, total calcite, percent of pixels containing coccolithophores (PPCC), SST, and PAR for September 1997–October 2005 (January 1997–December 2004 for SST). The total calcite (10^9 gC m^{-1}) was obtained from the product of calcite concentration and the area of each pixel and then summed over the entire regional polygon (Figure 1). Note that the Chl *a* starts rising every year around September and peaks around November, with a few exceptions (2001 and 2003) where the increase in Chl *a* started one or two months earlier. The calcite always reaches its peak after the maximum Chl *a* concentration has been reached, in accordance with the analysis of Figure 2. The time series of PPCC provides an independent evidence of the coccolithophore blooms and has interannual variability and timing remarkably similar to the calcite concentration. Also note that PAR leads SST by about 2 months, implying that light becomes available for the spring bloom before the MLD reaches a minimum value. Even though the timing of the phytoplankton blooms is almost always predictable, their intensity and duration are highly variable from year to year.

4. Summary and Conclusions

[11] We described environmental processes that drive the timing and duration of coccolithophore blooms along the

Table 1. Monthly Means of SST, SSS, MLD, Nitrate, Phosphate, and Silicate From Seasonal Climatology and PAR, Chl a, and PIC Derived From SeaWiFS Data

Month	SST, °C	SSS, psu	MLD, m	PAR, W/m^2	NO$_3$, μM	PO$_4$, μM	SiO$_2$, μM	Chl a, mg m^{-3}	PIC, mmol C m^{-3}
Jun	6.98	33.933	109.1	31.7	13.5	1.50	5.8	0.30	0.04
Jul	6.30	33.929	140.9	34.7	15.6	1.49	5.3	0.21	0.12
Aug	5.98	33.974	149.3	51.0	19.7	1.29	4.4	0.23	0.01
Sep	5.85	33.989	153.4	82.2	21.0	1.09	5.9	0.63	0.04
Oct	6.71	33.914	83.3	119.5	15.4	1.40	4.3	1.91	0.40
Nov	8.54	33.872	35.2	152.4	9.5	0.88	3.6	2.56	1.66
Dec	10.26	33.865	21.0	167.4	7.2	0.83	3.1	2.07	2.93
Jan	12.18	33.915	17.6	161.6	5.9	0.68	1.9	2.19	3.25
Feb	12.28	33.874	23.4	136.7	5.1	0.83	3.8	1.70	2.50
Mar	11.85	33.932	32.2	103.0	8.0	0.84	4.5	1.03	0.92
Apr	10.06	33.937	44.1	65.1	9.6	1.02	2.0	0.40	0.08
May	8.78	33.980	71.4	40.6	15.5	1.20	5.9	0.30	0.03
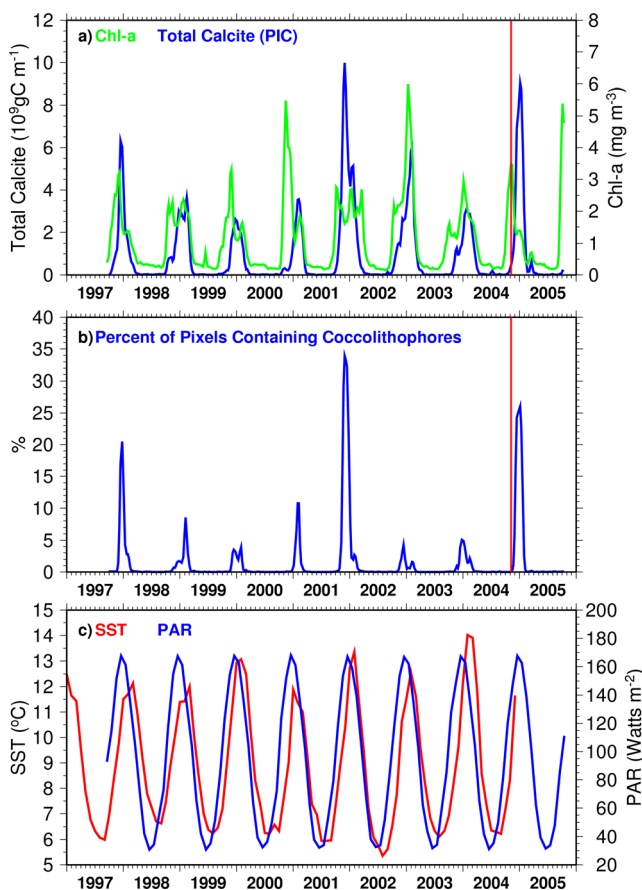
Figure 3. Time series of SeaWiFS-derived mean (a) chlorophyll, PIC, (b) percent of pixels containing coccolithophores, (c) PAR, and AVHRR SST for the regional domain of Figure 1. The vertical red line in Figures 3a and 3b corresponds to the time period of the Patagonian shelf-break cruise (November 2004).

of vertical stratification, and consequently the availability and proportion of nutrients within the euphotic layer, plays a role on driving the interannual changes.

Patagonian shelf break. The seasonal variability of these blooms responds to light intensity and nutrient supply changes within the mixed layer, which is in agreement with previous investigations in other locations. The early spring bloom is presumably diatom-dominated and starts in September under nutrient-rich upwelled Malvinas waters when the mixed layer begins to shallow (<80 m), and peaks around November when the MLD is less than 40 m. At this time the phytoplankton community is composed mainly of diatoms and dinoflagellates. After nutrients are depleted from the spring uptake, a coccolithophore bloom begins in November when the MLD is less than 40 m, and peaks in January when the MLD reaches its minimum (18 m) and PAR reaches its maximum intensity. This finding is consistent with earlier studies that identify maximum coccolithophore growth under well-illuminated shallow MLD and low phosphate concentrations, which are environmental conditions that limit the growth of diatoms and other groups.

[12] Although the ocean color data shows that the timing and location of the Patagonian shelf break bloom is very predictable from year to year, significant interannual variability was identified on the intensity of the bloom. Further oceanographic cruises are planned to investigate the causes of this interannual variability. We anticipate that the degree

References

Balch, W. M., R. W. Eppley, M. R. Abbott, and F. M. H. Reid (1989), Bias in satellite-derived pigment measurements due to coccolithophores and dinoflagellates, *J. Plankton Res.*, *11*(3), 575–581.

Balch, W. M., H. R. Gordon, B. C. Bowler, D. T. Drapeau, and E. S. Booth (2005), Calcium carbonate measurements in the surface global ocean based on Moderate-Resolution Imaging Spectroradiometer data, *J. Geophys. Res.*, *110*, C07001, doi:10.1029/2004JC002560.

Brand, L. E. (1991), Minimum iron requirements of marine phytoplankton and the implications for the biogeochemical control of new production, *Limnol. Oceanogr.*, *36*, 1756–1771.

Brown, C. W., and G. P. Podesta (1997), Remote sensing of coccolithophore blooms in the western South Atlantic Ocean, *Remote Sens. Environ.*, *60*(1), 83–91.

Carreto, J. I., V. A. Lutz, M. O. Carignan, A. D. C. Colleoni, and S. G. Demarco (1995), Hydrography and chlorophyll-a in a transect from the coast to the shelf-break in the Argentinian Sea, *Cont. Shelf Res.*, *15*(2–3), 315–336.

Conkright, M. E., R. A. Locarnini, H. E. Garcia, T. D. O'Brien, T. P. Boyer, C. Stephens, and J. I. Antonov (2002), World ocean atlas 2001: Objective analyses, data statistics, and figures, CD-ROM documentation, *Internal Rep. 17*, 17 pp., Natl. Oceanogr. Data Cent., Silver Spring, Md.

Frouin, R., D. W. Lingner, C. Gautier, K. S. Baker, and R. C. Smith (1989), A simple analytical formula to compute clear sky total and photosynthetically available solar irradiance at the ocean surface, *J. Geophys. Res.*, *94*(C7), 9731–9742.

Gayoso, A. M. (1995), Bloom of Emiliania-huxleyi (Prymnesiophyceae) in western South Atlantic Ocean, *J. Plankton Res.*, *17*(8), 1717–1722.

Glorioso, P. D., and R. A. Flather (1997), The Patagonian shelf tides, *Prog. Oceanogr.*, *40*(1–4), 263–283.

Gordon, H. R., G. C. Boynton, W. M. Balch, S. B. Groom, D. S. Harbour, and T. J. Smyth (2001), Retrieval of coccolithophore calcite concentration from SeaWiFS imagery, *Geophys. Res. Lett.*, *28*(8), 1587–1590.

Heimdal, B. R., J. K. Egge, M. J. W. Veldhuis, and P. Westbroek (1994), The 1992 Norwegian emiliania-huxleyi experiment—An overview, *Sarsia*, *79*(4), 285–290.

Hentschel, E. (1932), Wissenschaftliche Ergebnisse der deutschen Atlantischen Expedition "Meteor" 1925–1927, in *Die Biologischen Methoden und Biologische Beobachtungsmaterial der Meteor Expedition*, Wiss. Ergeb. Dtsch. Atl. Exped. Meteor 1925–1927, 10, pp. 275.

Holligan, P. M., et al. (1993a), A biogeochemical study of the coccolithophore, *Emiliania huxleyi*, in the North Atlantic, *Global Biogeochem. Cycles*, *7*(4), 879–900.

Holligan, P. M., S. B. Groom, and D. S. Harbour (1993b), What controls the distribution of the coccolithophore, Emiliania huxleyi, in the North Sea?, *Fish. Oceanogr.*, *2*, 175–183.

Iglesias-Rodríguez, M. D., C. W. Brown, S. C. Doney, J. Kleypas, D. Kolber, Z. Kolber, P. K. Hayes, and P. G. Falkowski (2002), Representing key phytoplankton functional groups in ocean carbon cycle models: Coccolithophorids, *Global Biogeochem. Cycles*, *16*(4), 1100, doi:10.1029/2001GB001454.

Levitus, S. E. (1982), Climatological atlas of the world ocean, *NOAA Prof. Pap. 13*, US Gov. Print. Off., Washington, D. C.

Margalef, R. (1978), Life-forms of phytoplankton as survival alternatives in an unstable environment, *Oceanol. Acta*, *1*(4), 493–509.

O'Reilly, J. E., et al. (2000), SeaWiFS postlaunch technical report series, Volume 11, SeaWiFS postlaunch calibration and validation analyses, Part 3, *NASA/TM-2000–206892*, edited by S. B. Hooker and R. R. Firestone, 49 pp., NASA Goddard Space Flight Center, Greenbelt, Md.

Patt, F. S., et al. (2003), SeaWiFS postlaunch technical report series, Volume 22, Algorithm updates for the fourth SeaWiFS data reprocessing, *NASA/TM-2003–206892*, 74 pp., NASA Goddard Space Flight Center, Greenbelt, Md.

Piola, A. R., and R. P. Matano (2001), Brazil and Falklands (Malvinas) currents, in *Encyclopedia of Ocean Sciences*, edited by S. A. Thorpe, pp. 340–349, Elsevier, New York.

Romero, S. I., A. R. Piola, M. Charo, and C. A. E. Garcia (2006), Chlorophyll-a variability off Patagonia based on SeaWiFS data, *J. Geophys. Res.*, *111*, C05021, doi:10.1029/2005JC003244.

Saraceno, M., C. Provost, and A. R. Piola (2005), On the relationship between satellite-retrieved surface temperature fronts and chlorophyll *a* in the western South Atlantic, *J. Geophys. Res.*, *110*, C11016, doi:10.1029/2004JC002736.

Smyth, T. J., T. Tyrrell, and B. Tarrant (2004), Time series of coccolithophore activity in the Barents Sea, from twenty years of satellite imagery, *Geophys. Res. Lett.*, *31*, L11302, doi:10.1029/2004GL019735.

Townsend, D. W., M. D. Keller, P. M. Holligan, S. G. Ackleson, and W. M. Balch (1994), Blooms of the coccolithophore Emiliania-huxleyi with respect to hydrography in the Gulf of Maine, *Cont. Shelf Res.*, *14*(9), 979–1000.

Tyrrell, T., and A. H. Taylor (1995), Latitudinal and seasonal variations in carbon dioxide and oxygen in the northeast Atlantic and the effects on *Emiliania huxleyi* and other phytoplankton, *Global Biogeochem. Cycles*, *9*(4), 585–604.

Tyrrell, T., and A. Merico (2004), Emiliania huxleyi: Bloom observations and the conditions that induce them, in *Coccolithophores: From Molecular Processes to Global Impact*, edited by J. R. Young, pp. 75–97, Springer, New York.

————————————

C. A. E. Garcia and M. M. Mata, Department of Physics, Federal University of Rio Grande, Rua Engenheiro Alfredo Huch 475, Rio Grande, RS 96201-900, Brazil.

V. M. T. Garcia, Department of Oceanography, Federal University of Rio Grande, Avenida Italia, Km 8, Rio Grande, RS 96201-900, Brazil.

C. R. McClain, NASA Goddard Space Flight Center, Code 614.8, Greenbelt, MD 20771, USA.

A. R. Piola, Servicio de Hidrografia Naval and Universidad de Buenos Aires, Avenida Montes de Oca 2124, Buenos Aires, Capital Federal C1270ABV, Argentina.

S. R. Signorini, SAIC, NASA Earth Sciences Support, NASA Goddard Space Flight Center, 4600 Powder Mill Road, Beltsville, MD 20705-2675, USA. (sergio@simbios.gsfc.nasa.gov)